

# A Simple Baseline for Spoken Language to Sign Language Translation with 3D Avatars

Ronglai Zuo<sup>1\*</sup> Fangyun Wei<sup>2\*†</sup> Zenggui Chen<sup>2</sup> Brian Mak<sup>1</sup> Jiaolong Yang<sup>2</sup> Xin Tong<sup>2</sup>  
<sup>1</sup>The Hong Kong University of Science and Technology <sup>2</sup>Microsoft Research Asia  
 {rzuo,mak}@cse.ust.hk {fawe,v-zenchen,jiaoyan,xtong}@microsoft.com



Figure 1. (a) Previous works have primarily focused on translating sign languages into spoken languages (Sign2Spoken). (b) Our work is the first to facilitate translation from spoken languages to sign languages (Spoken2Sign), utilizing a 3D avatar to display the translation results.

## Abstract

The objective of this paper is to develop a functional system for translating spoken languages into sign languages, referred to as Spoken2Sign translation. The Spoken2Sign task is orthogonal and complementary to traditional sign language to spoken language (Sign2Spoken) translation. To enable Spoken2Sign translation, we present a simple baseline consisting of three steps: 1) creating a gloss-video dictionary using existing Sign2Spoken benchmarks; 2) estimating a 3D sign for each sign video in the dictionary; 3) training a Spoken2Sign model, which is composed of a Text2Gloss translator, a sign connector, and a rendering module, with the aid of the yielded gloss-3D sign dictionary. The translation results are then displayed through a sign avatar. As far as we know, we are the first to present the Spoken2Sign task in an output format of 3D signs. In addition to its capability of Spoken2Sign translation, we also demonstrate that two by-products of our approach—3D keypoint augmentation and multi-view understanding—can assist in keypoint-based sign language understanding. Code and models will be available at <https://github.com/FangyunWei/SLRT>.

## 1. Introduction

Sign languages are the primary means of communication for the deaf. Numerous previous works [8, 9, 39, 68, 69,

74] have focused on sign language translation, with the goal of translating sign languages into spoken languages (Sign2Spoken, Figure 1a). However, this paper shifts the focus to the reverse process: translating spoken languages into sign languages (Spoken2Sign, Figure 1b) to further bridge the communication gap between the deaf and the hearing.

A majority of prior works [25–27, 52, 53, 56, 60, 65] on Spoken2Sign translation (aka sign language production) focused on expressing translation outcomes through keypoints. However, the keypoint representations often pose interpretable challenges for signers [50]. With the evolution of generative models [2, 71], several studies [16, 57, 59] have employed these keypoints to animate sign images, subsequently creating a sign video. However, the 2D video format is prone to blurriness and visual distortions. In this work, we introduce an innovative method for Spoken2Sign translation by utilizing a 3D avatar to represent the translation results. In contrast to earlier attempts that utilized generative models [51, 58], our method prioritizes enhancing understandability and incorporates a 3D human pose prior with a special emphasis on signing poses, allowing for multi-view representations of the translation results.

We begin with the basic concepts of sign languages:

- *Isolated sign*. An isolated sign is a single gesture comprising handshapes, along with movements of the body and hands. Sometimes, facial expressions also play a role in conveying information.
- *Continuous sign*. It is a sequence of several isolated signs.

\*Equal contribution.

†Corresponding author.

- *Co-articulation*. It refers to the movement of the hands and body between two adjacent signs in a continuous sign.
- *Gloss*. A gloss refers to the label assigned to a specific isolated sign. It is usually represented as a word or phrase.
- *Gloss sequence*. A label sequence for a continuous sign. In our system, it serves as an intermediate representation.
- *Text*. It refers to the translation of a continuous sign. Generally, the *gloss sequence* does not equate the *text*, as the linguistic rules (*e.g.*, word order) between a sign language and its corresponding spoken language can be different.

As shown in Figure 2, our Spoken2Sign translation baseline includes three steps: 1) dictionary construction; 2) 3D sign estimation for each entry in the dictionary; and 3) Spoken2Sign translation in a retrieve-then-connect paradigm.

**Dictionary Construction.** As shown in Figure 2a, we initially create a gloss-video dictionary comprising  $M$  glosses, each of which may contain multiple isolated sign videos that express the same meaning. Existing sign language recognition (SLR) datasets are typically divided into: 1) datasets for isolated SLR (ISLR), *e.g.*, WLASL [38] and MSASL [31]; 2) datasets for continuous SLR (CSLR), *e.g.*, Phoenix-2014T [4] and CSL-Daily [76]. The objective of this work is to develop a Spoken2Sign system, that translates the input text into a sequence of 3D signs, using glosses as intermediate representations. Although existing ISLR datasets are inherent sign language dictionaries, they lack parallel text-gloss sequence data, posing a challenge for the essential text-to-gloss sequence translation. An alternative is to leverage the CSLR datasets; nevertheless, these datasets do not include a dictionary. Fortunately, a CSLR model trained with the connectionist temporal classification (CTC) loss [19] is capable to effectively segment a continuous sign video into a collection of isolated signs [63]. In this paper, for the purpose of segmenting continuous signs into isolated ones to construct a dictionary, we adopt the state-of-the-art CSLR model, TwoStream-SLR [9], as the sign segmentor.

**3D Sign Estimation.** We currently have a gloss-video dictionary at our disposal. Our next step converts each sign video within this dictionary into a 3D sign. This transformation is essential to mimicing co-articulations more naturally and stitching two signs together in 3D space during Spoken2Sign translation. Inspired by recent advances in 3D whole-body parametric models and monocular 3D whole-body reconstruction [30, 49, 66], we introduce a sign-language-specific version of SMPLify-X [49]: SMPLSign-X. This approach is dedicated to estimating 3D signs from monocular sign videos. The vanilla SMPLify-X estimates a holistic and expressive 3D human representation by optimizing shape, pose, and expression parameters. To enhance its application to 3D sign estimation, we incorporate a series of improvements including promoting temporal consistency and involving a more effective 3D pose prior tailored for sign language avatars. Following these improvements, we construct a gloss-3D sign

dictionary. The entire process is depicted in Figure 2b.

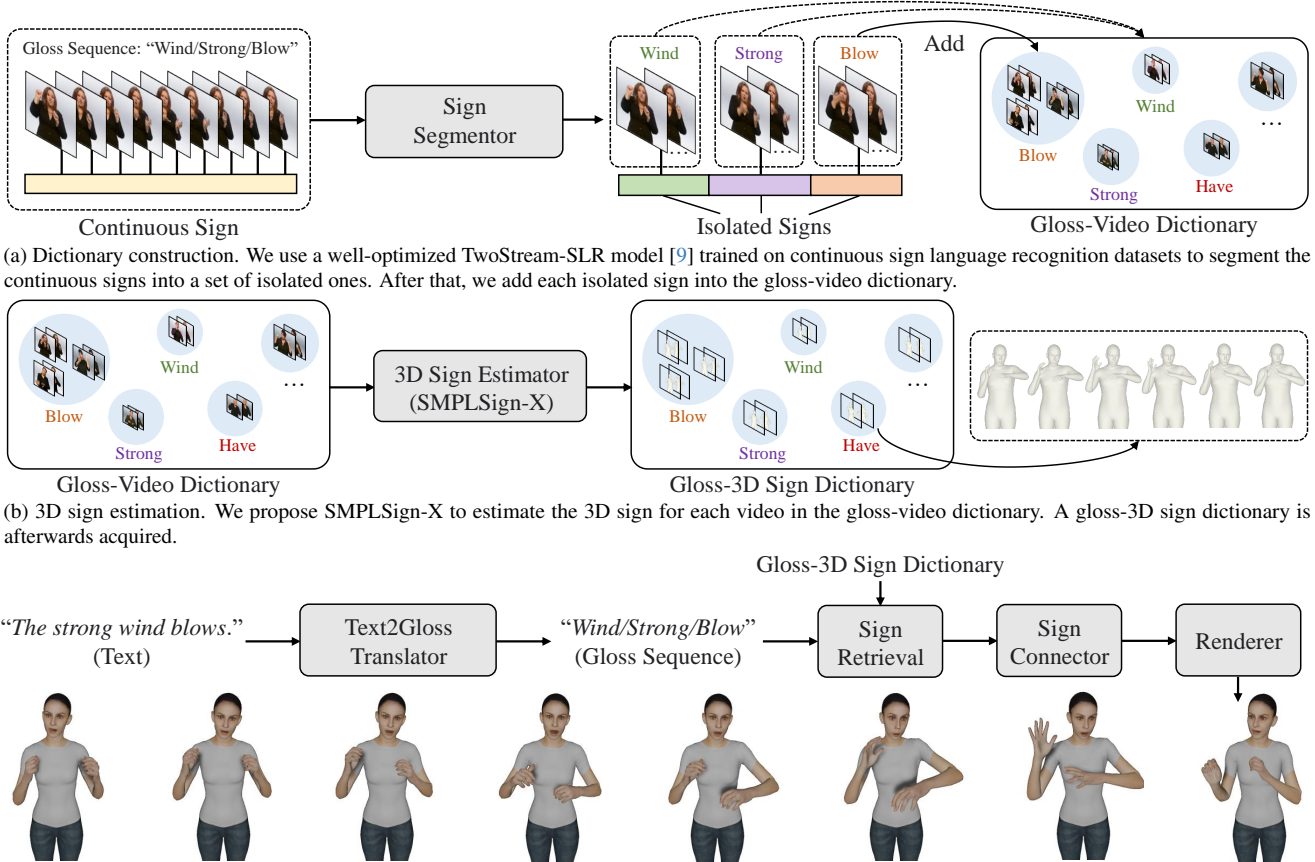
**Spoken2Sign Translation.** Figure 2c illustrates the core idea behind the proposed Spoken2Sign translation. Glosses serve as a link between sign languages and spoken languages. Therefore, training a text-to-gloss-sequence (Text2Gloss) model is necessary to enable Spoken2Sign translation. Following [7, 9], we adopt mBART [42] as our Text2Gloss model due to its promising sequence-to-sequence translation capability. For each gloss in the gloss sequence, we retrieve its corresponding 3D sign from the gloss-3D sign dictionary. A significant challenge arises in seamlessly stitching two adjacent signs, as it is crucial to imitate the co-articulations between them to produce visually appealing translation results. To address this challenge, we develop a sign connector that predicts the duration of each co-articulation. Our experiments reveal that this simple sign connector surpasses the baseline which uses a fixed duration instead. The final translation results are obtained by rendering the output of the sign connector as a sign avatar.

In summary, the contributions of this work are:

- We present a simple yet effective baseline for Spoken2Sign translation. To the best of our knowledge, this is the first work of developing a practical Spoken2Sign system that utilizes a 3D avatar to display the translation results.
- Considering the unique characteristics of sign languages, we propose SMPLSign-X, a novel method for 3D sign estimation. Our method aims to develop comprehensive 3D sign language dictionaries for well-established benchmarks including Phoenix-2014T and CSL-Daily. We will release these dictionaries to facilitate future research.
- Our Spoken2Sign system sets a new state-of-the-art performance in back-translation evaluation.
- Besides demonstrating the capability of Spoken2Sign translation, we also show that two by-products of our approach significantly enhance keypoint-based models for sign language understanding.

## 2. Related Work

**Sign Language Understanding.** There are several research directions in sign language understanding, such as sign language recognition (SLR), sign language translation (SLT), sign spotting [1, 45, 46, 61], and sign language retrieval [11, 15]. The objective of SLR is to transcribe a sign video into its constituent glosses. It can be categorized into isolated SLR (ISLR) [21, 22, 28, 31, 38, 40, 72, 80] and continuous SLR (CSLR) [8–10, 20, 23, 44, 73, 75, 78, 79]. The former is a classification task aimed at predicting the gloss of an isolated sign, while the latter focuses on recognizing a sequence of signs in a video and generating the corresponding gloss sequence. SLT takes a step further—it aims at translating sign languages into spoken languages. Existing works [4–6, 8, 9, 40, 70, 76, 77] attempt to formulate the SLT task as a neural machine translation problem, using a visual encoder



(a) Dictionary construction. We use a well-optimized TwoStream-SLR model [9] trained on continuous sign language recognition datasets to segment the continuous signs into a set of isolated ones. After that, we add each isolated sign into the gloss-video dictionary.

(b) 3D sign estimation. We propose SMPLSign-X to estimate the 3D sign for each video in the gloss-video dictionary. A gloss-3D sign dictionary is afterwards acquired.

(c) Spoken2Sign translation. We first employ a sequence-to-sequence network mBART [9, 42] to convert the input text into the intermediate representation, *i.e.*, gloss sequence. We then retrieve the corresponding 3D sign for each gloss in the gloss sequence. A sign connector is trained to generate the co-articulation between two adjacent 3D signs. Finally, we render the output and display the translation results through a 3D avatar.

Figure 2. Overview of our methodology. It consists of (a) dictionary construction; (b) 3D sign estimation; (c) Spoken2Sign translation. Sign videos are from Phoenix-2014T [4], a German sign language benchmark. We translate German into English to ease comprehension.

and a language model. Inspired by the recent success of transferring a pre-trained language model to SLT [9], we adopt mBART [42] as our Text2Gloss translator.

**Spoken2Sign Translation.** In contrast to sign language understanding, this area remains under-explored. Almost all previous works [24–27, 52, 53, 56, 60, 65] focus on expressing translation results through keypoints, which are often difficult for signers to understand [50]. With the advances of generative models, several studies [14, 16, 57, 59] leverage these keypoints to animate sign language videos. However, these approaches often encounter challenges such as blurriness and visual distortions. Some papers [34, 43] proposed the use of avatars to display sign languages, but they were too early to benefit from the advanced parametric 3D human models [49]. In contrast, our approach incorporates a 3D signer pose prior, enhancing both the understandability and the temporal consistency of the animations.

**3D Whole-Body Estimation.** Recent monocular 3D whole-body estimation approaches adopt parametric models such as Frank [30] and SMPL-X [49] for 3D body representation. These approaches can be divided into fitting-based

and regression-based methods. The former utilizes optimization algorithms to fit the parametric model to the given 2D observations, such as body keypoints and segmentation masks [36, 49, 64, 66]. In contrast, the latter directly predicts model parameters without iterative optimization [3, 32, 41, 67], although they often rely on precise SMPL-X annotations [3]. Parametric models have also been applied in sign language research [17, 21, 22, 37]. However, none of these studies have developed a complete Spoken2Sign pipeline. In this work, we tailor the widely-used SMPL-X parametric model by incorporating sign-language-specific priors for monocular 3D sign estimation and introduce a functional system for Spoken2Sign translation.

### 3. Methodology

This section details our methodology, which comprises three stages: dictionary construction (Section 3.1), 3D sign estimation (Section 3.2), and Spoken2Sign translation (Section 3.3). Additionally, we discuss two by-products derived from 3D signs in Section 3.4. An overview is depicted in Figure 2.

### 3.1. Dictionary Construction

Our Spoken2Sign system is built upon the availability of a sign dictionary, which consists of gloss-video pairs. Nevertheless, existing datasets [4, 76] do not provide such dictionaries. Inspired by the capability of a well-trained CSLR model to segment a continuous sign video into a collection of isolated signs by finding the optimal alignment path [13, 63] through the dynamic time warping (DTW) algorithm [47], we adopt the state-of-the-art CSLR model, TwoStream-SLR [9], as the sign segmentor. This model is used to build a sign dictionary containing the segmented isolated signs for each dataset, as shown in Figure 2a. Subsequently, we acquire a sign dictionary containing  $M$  glosses. We also generate a set of co-articulations (which are transitions between two adjacent signs, corresponding to the blank class in the CTC loss [19]) to train our sign connector. More details can be found in the supplementary materials.

### 3.2. 3D Sign Estimation

We introduce the process of estimating the 3D representation for each isolated sign (*i.e.*, a monocular video) in the dictionary, as shown in Figure 2b.

**Preliminaries of SMPLify-X and SMPL-X.** SMPLify-X [49] is a widely used method to estimate a 3D representation of human body pose, hand pose, and facial expression from a single monocular image. The yielded 3D human representation is termed as a SMPL-X model [49], which is defined by a series of learnable parameters. These parameters include global orientation  $\zeta \in \mathbb{R}^3$ , body shape  $\beta \in \mathbb{R}^{10}$ , facial expression  $\psi \in \mathbb{R}^{10}$ , and body pose  $\theta \in \mathbb{R}^{3N}$ , where  $N = 54$  denotes the number of joints. Note that pose parameters represent the relative axis-angle rotations to the parent joints defined in a kinematics map. Using these parameters, the SMPL-X model could produce a mesh comprising 10,475 vertices and a set of 118 3D joints  $\mathcal{D} \in \mathbb{R}^{118 \times 3}$ . For simplicity, we use  $\mathcal{D}_i \in \mathbb{R}^3$  ( $1 \leq i \leq 118$ ) to denote the  $i$ -th joint in  $\mathcal{D}$ . Note that only 54 out of the 118 joints are associated with the pose parameters  $\theta$ .

To fit the SMPL-X model to a single monocular image, we first use HRNet [62] pre-trained on COCO-Wholebody [29], to estimate the image’s 2D keypoints  $\mathcal{K} \in \mathbb{R}^{118 \times 2}$ . We employ only a subset of the COCO-Wholebody keypoints for aligning the joints defined by SMPL-X. Subsequently, SMPLify-X [49] seeks to minimize the following objective function by optimizing  $\zeta$ ,  $\beta$ ,  $\psi$  and  $\theta$ :

$$\mathcal{L} = \mathcal{L}_{joint} + \mathcal{L}_{prior} + \mathcal{L}_{penetration}, \quad (1)$$

where  $\mathcal{L}_{joint}$  is the major loss function that minimizes the distance between the 2D keypoints  $\mathcal{K}$  and the projected keypoints  $P(\mathcal{D})$ ;  $\mathcal{L}_{prior}$  denotes a combination of losses that incorporate prior knowledge of hand pose, facial pose, body shape, and facial expressions, and penalize extreme body states;  $\mathcal{L}_{penetration}$  is a regularization term designed

to prevent the SMPL-X model from penetrations and self-collisions. In SMPLify-X,  $\mathcal{L}_{joint}$  is formulated as:

$$\mathcal{L}_{joint} = \frac{1}{|\mathcal{J}|} \sum_{i \in \mathcal{J}} \gamma_i \omega_i \ell_r(P(\mathcal{D}_i) - \mathcal{K}_i), \quad (2)$$

where  $\mathcal{J}$  represents the set of 118 3D joints;  $P(\cdot)$  is a function that projects each 3D joint  $\mathcal{D}_i \in \mathbb{R}^3$  from the world coordinate to image coordinate;  $\mathcal{K}_i$  is the associated 2D keypoint (pseudo ground truth) of  $\mathcal{D}_i$ ;  $\omega_i$  is the confidence (yielded by HRNet) of  $\mathcal{K}_i$ ;  $\gamma_i$  is the pre-defined weight of joint  $\mathcal{D}_i$ ;  $\ell_r$  represents a robust Geman-McClure loss function [18]. More details can be found in the SMPL-X paper [49].

**SMPLSign-X.** We enhance SMPLify-X by adapting its input from a single monocular *image* to a sign *video*. Additionally, we consider the unique properties of sign languages to further improve estimation quality. The upgraded version is named SMPLSign-X. Our improvements are based on three observations: 1) Optimization targets are absent for joints that do not appear in sign videos (*e.g.*, the lower body and a dropping hand); 2) The upper body of a signer remains upright during signing; 3) Independently fitting each frame to the SMPL-X model results in temporal inconsistencies and visually unsatisfactory outcomes. To address these issues, we define the objective function for SMPLSign-X as:

$$\mathcal{L} = \mathcal{L}_{joint} + \mathcal{L}_{prior} + \mathcal{L}_{penetration} + \lambda_1 \mathcal{L}_{unseen} + \lambda_2 \mathcal{L}_{upright} + \lambda_3 \mathcal{L}_{smooth}. \quad (3)$$

$\mathcal{L}_{unseen}$  (Eq. 4) is a regularization term that pushes the unseen keypoints to approach those of the rest pose. We use confidence scores predicted by the pre-trained HRNet to identify the unseen keypoints. Concretely, for a 2D keypoint  $\mathcal{K}_i$  and its confidence score  $\omega_i$ , we regard  $\mathcal{K}_i$  as an unseen keypoint if  $\omega_i < \lambda$ , where  $\lambda$  is a pre-defined threshold,  $\lambda = 0.65$  by default. SMPLify-X provides joint mappings between the 2D keypoints  $\mathcal{K}$  and the pose parameters  $\theta$ . Therefore, we can easily identify the set of unseen joints ( $\mathcal{J}_{unseen}$ ) in the  $\theta$  space. We use  $\hat{\theta}$  to denote the pose parameters of the rest pose, which are frozen during training.

$$\mathcal{L}_{unseen} = \sum_{i \in \mathcal{J}_{unseen}} \ell_r(\theta_i - \hat{\theta}_i). \quad (4)$$

$\mathcal{L}_{upright}$  (Eq. 5) denotes a regularization term for encouraging an upright posture in the upper body. To accomplish this, we define a keypoint set  $\mathcal{J}_{upright}$ , including the neck and pelvis keypoints within the context of  $\theta$  space. Our goal is to preserve depth consistency across all keypoints in  $\mathcal{J}_{upright}$ , as specified by the loss in Eq. 5, where  $d$  represents depth.

$$\mathcal{L}_{upright} = \sum_{i,j \in \mathcal{J}_{upright}} \ell_r(d_i - d_j). \quad (5)$$

Finally, given the pose parameters  $\theta_i^{pre}$  of the previous frame, we use Eq. 6 to preserve the temporal consistency for the

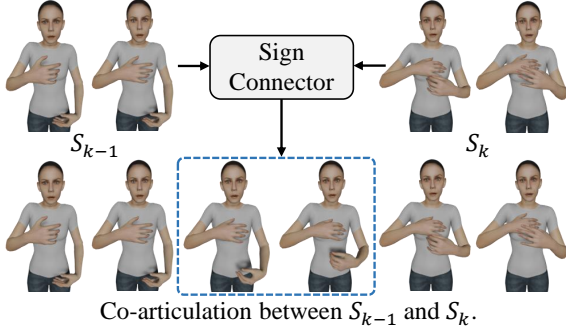


Figure 3. Illustration of the sign connector. The objective is to predict the duration of the co-articulation between two adjacent 3D signs,  $S_{k-1}$  and  $S_k$ , followed by generating the co-articulation through interpolation in the 3D joint space.

current frame.  $\mathcal{J}_\theta$  is the set containing all joints in the  $\theta$  space.  $\gamma_i$  denotes the weight of the  $i$ -th joint. These joint weights are pre-defined by SMPLify-X [49].

$$\mathcal{L}_{smooth} = \sum_{i \in \mathcal{J}_\theta} \gamma_i \ell_r(\theta_i - \theta_i^{pre}). \quad (6)$$

We estimate the 3D representation for each sign video from the gloss-video dictionary using the objective function in Eq. 3, on a frame-by-frame basis. Subsequently, we construct a gloss-3D sign dictionary.

### 3.3. Spoken2Sign Translation

As shown in Figure 2c, our Spoken2Sign translation pipeline primarily consists of three components: 1) a Text2Gloss translator that translates the input text into a gloss sequence; 2) a sign connector, which stitches two adjacent 3D signs together; and 3) a rendering module, which produces the final animated sign avatar.

**Text2Gloss Translator.** Inspired by the recent success of sign language translation (SLT) [9], we adopt mBART [42] as our Text2Gloss translator. Existing SLT benchmarks [4, 76] typically provide annotations of text-gloss-sequence pairs. In the vein of traditional SLT models, which train a Gloss2Text network using gloss sequences as inputs and texts as outputs, we train a Text2Gloss translator by simply reversing the inputs and outputs. Our Text2Gloss translator achieves a promising BLEU-4 score of 29.27/31.88 on the dev set of Phoenix-2014T/CSL-Daily. More details are available in the supplementary materials.

**Sign Retrieval.** For each gloss predicted by the Text2Gloss translator, we retrieve its corresponding 3D sign from the gloss-3D sign dictionary. Since a single gloss may be associated with multiple 3D signs, we develop a retrieval strategy to identify the optimal one. Specifically, we train an ISLR model [80] on all instances in the dictionary. During retrieval, we feed candidate signs into the ISLR model and select the sign with the highest confidence for the gloss query.

**Sign Connector.** As shown in Figure 3, we present a sign connector to predict the duration of co-articulation between two adjacent 3D signs when they are stitched together. As described in Section 3.1, we generate a set of co-articulations, each of which is denoted as a triplet  $(\mathcal{D}_{\mathcal{J}_{SC}}^{pre}, L, \mathcal{D}_{\mathcal{J}_{SC}}^{next})$ , where  $L$  is the duration of the co-articulation,  $\mathcal{J}_{SC}$  denotes the set of 3D joints used in our sign connector, and  $\mathcal{D}_{\mathcal{J}_{SC}}^{pre}$  and  $\mathcal{D}_{\mathcal{J}_{SC}}^{next}$  represent the 3D joints of the preceding and succeeding signs of the co-articulation, respectively. In our implementation,  $\mathcal{J}_{SC}$  includes the joints of hands, wrists, and elbows. Our sign connector is a 4-layer MLP taking the concatenation of  $\mathcal{D}_{\mathcal{J}_{SC}}^{pre}$ ,  $\mathcal{D}_{\mathcal{J}_{SC}}^{next}$ , and their Euclidean coordinate distance  $\mathcal{D}_{\mathcal{J}_{SC}}^{pre} - \mathcal{D}_{\mathcal{J}_{SC}}^{next}$  as inputs. We minimize the loss between the prediction yielded by the MLP and the target  $L$  using the L1 loss function.

Once the sign connector is optimized, given a 3D sign sequence  $\{S_1, S_2, \dots, S_{K-1}, S_K\}$ , it can predict the duration  $\hat{L}_k$  of the co-articulation between two adjacent 3D signs  $S_{k-1}$  and  $S_k$  ( $2 \leq k \leq K$ ). Subsequently, we interpolate  $\hat{L}_k$  frames between the last frame of  $S_{k-1}$  and the first frame of  $S_k$  in the parameter space to simulate the co-articulation  $C_k^{\hat{L}_k}$ . Finally, a 3D sign sequence  $\{S_1, C_2^{\hat{L}_2}, S_2, \dots, S_{K-1}, C_{K-1}^{\hat{L}_{K-1}}, S_K\}$  is yielded for rendering.

**Rendering Module.** We render the 3D sign sequence frame by frame using the Blender toolkit [12]. The pose and facial expression parameters of the SMPL-X model are utilized to drive the avatar.

### 3.4. By-Products of 3D Signs

The generated 3D signs implicitly integrate the human pose prior within the SMPLSign-X. Below, we discuss two by-products of these 3D signs, which significantly enhance keypoint-based models for sign language understanding.

**3D Keypoint Augmentation.** In contrast to existing Spoken2Sign translation works [52, 53, 55–57], which only generate frontal-view keypoints/videos, our approach outputs a sequence of 3D signs. The 3D nature of these signs allows the development of 3D keypoint augmentation to enhance keypoint-based models for sign language understanding. Specifically, during each training iteration, we sample an angle,  $\delta$ , from a pre-defined range of  $[-\Delta, \Delta]$ , where  $\Delta = 20^\circ$  by default. We then rotate the original 3D keypoints by  $\delta$ , modifying the global orientation parameters  $\zeta$ . Finally, the projected 2D keypoints are fed into the sign language understanding models as inputs.

**Understanding from Multiple Views.** Current datasets for sign language understanding commonly include 2D videos of signs captured from a frontal perspective. This limitation leads to the development of models that are only capable of interpreting sign languages from this single viewpoint. The introduction of 3D signs naturally enables sign language understanding from multiple views. Drawing inspiration from the TwoStream Network [9], which simultaneously



Figure 4. Qualitative results on Phoenix-2014T [4] (a and b) and CSL-Daily [76] (c). In each sub-figure, we display the text in the caption, and show the ground truth sign video and our translation result in the first row and second row, respectively.

processes 2D sign videos and their corresponding keypoint sequences, we modify the network to process two keypoint sequences: one sequence represents the original frontal view (a projection of the 3D keypoints without rotation), while the other sequence represents the side view (a projection of the 3D keypoints resulted from a  $60^\circ$  rotation).

## 4. Experiments

**Datasets and Evaluation Metrics.** Due to the absence of SMPL-X annotations in existing sign language datasets, we evaluate our Spoken2Sign system using the widely-adopted back-translation metric [55–57] on Phoenix-2014T (P-2014T) [4] and CSL-Daily (CSL) [76]. P-2014T is a

Method	Dev		Test	
	BLEU-4	ROUGE	BLEU-4	ROUGE
PT [52]	11.82	33.18	10.51	32.46
AT [53]	12.65	33.68	10.81	32.74
MDN [55]	11.54	33.40	11.68	33.19
MoMP [56]	14.03	37.76	13.30	36.77
FS-Net [57]	16.92	35.74	21.10	42.57
SignDiff [16]	18.26	39.62	22.15	46.82
Ours	<b>24.16</b>	<b>49.12</b>	<b>25.46</b>	<b>49.68</b>

Table 1. Comparison of back-translation performance with existing Spoken2Sign translation works on the Phoenix-2014T benchmark.

German sign language dataset with a vocabulary size of 1,066 for glosses and 2,887 for German text and there are 7,096/519/642 samples in its training/dev/test set. CSL is a large-scale Chinese sign language dataset, consisting of 18,401/1,077/1,176 samples in the training/dev/test set. Its vocabulary includes 2,000 glosses and 2,343 Chinese words. Following [55–57], we report BLEU-4 and ROUGE-L scores. In the P-2014T and CSL datasets, signers are recorded while standing stationary in front of the camera, maintaining an almost fixed pose. To verify the effectiveness of 3D keypoint augmentation, we conduct classification experiments on two extra datasets, WLASL [38] and MSASL [31], which feature more pronounced variations in signer poses. We report per-instance/class top-1/5 accuracy [80].

**Implementation Details.** Following SMPLify-X [49], we optimize Eq. 3 for multiple stages with the Limited-memory BFGS optimizer (L-BFGS) [48]. By default, we set  $\lambda_1 = 3e5$ ,  $\lambda_2 = 7e5$ , and  $\lambda_3 = 1e3$ , in Eq. 3. Each frame takes 300 epochs to fit the SMPL-X model [49]. To better keep temporal consistency, we pre-estimate the unified shape parameters  $\beta$  and global orientation  $\zeta$  of SMPL-X and extrinsic camera parameters for the input sign video. When training the sign connector, we set the learning rate as  $1e-5$  and use an Adam optimizer [33]. We filter out extreme samples with too long co-articulations for stable training. For a fair comparison with existing works [52, 53, 55–57], the inputs of all models are the re-projected 2D keypoints.

#### 4.1. Qualitative Evaluation

The objective of this work is to translate spoken languages into sign languages. The translation results are displayed through a 3D avatar. To verify the effectiveness of our system, we show several qualitative results on Phoenix-2014T and CSL-Daily in Figure 4. It can be seen that the translation results are aesthetically comparable to the ground truth sign videos. Refer to the supplementary materials for more qualitative results.

#### 4.2. Quantitative Evaluation

We employ the widely adopted back-translation metric [57] to assess the effectiveness of our 3D sign estimator. The estimated 3D signs consist of meshes and 3D keypoints. For

Dataset	Method	Dev		Test	
		BLEU-4	ROUGE	BLEU-4	ROUGE
P-2014T	HRNet [62]	22.94	48.81	24.95	49.13
	SMPLify-X [49]	19.21	44.28	19.69	43.65
	SMPLer-X* [3]	19.49	44.95	20.01	44.93
	OSX* [41]	22.31	47.71	23.00	47.23
	Ours	<b>24.16</b>	<b>49.12</b>	<b>25.46</b>	<b>49.68</b>
CSL	HRNet [62]	22.14	51.02	21.29	50.97
	SMPLify-X [49]	19.31	46.46	18.96	46.71
	SMPLer-X* [3]	20.76	48.93	20.86	49.29
	OSX* [41]	20.44	49.00	20.29	49.60
	Ours	<b>21.66</b>	<b>49.69</b>	<b>21.44</b>	<b>49.80</b>

Table 2. Comparison with other state-of-the-art 3D sign estimation methods using back-translation. We re-implement SMPLify-X [49], SMPLer-X [3] and OSX [41]. “HRNet” denotes a strong baseline that directly estimates 2D keypoints (pseudo ground truth) from raw videos. \*: regression-based methods trained on large-scale 3D datasets with SMPL-X annotations.

a fair comparison with previous works, we project these 3D keypoints back into 2D space, adopting a frontal view. Then, a Sign2Spoken model is trained using these re-projected 2D keypoint sequences to translate sign languages into spoken languages.

**Comparison with State-of-the-Art Works.** Table 1 presents a comparative analysis of our approach against other state-of-the-art works, focusing on back-translation. The prevalent approach in existing works [16, 52, 53, 55–57] uses generated keypoint sequences to represent sign languages. Additionally, some studies [16, 57] incorporate a GAN [54] or a Diffusion model [71] to further generate synthetic 2D videos from these keypoints. In contrast, our novel Spoken2Sign system produces a 3D sign sequences, visualized through an avatar. In line with the common practice, where back-translation is utilized for evaluation, our approach attains a BLEU-4 score of 24.16 on the Phoenix-2014T dev set, surpassing the previously best-performing method [16] by 5.9 points.

**3D Sign Estimator.** In Section 3.2, we present SMPLSign-X, an enhancement of the vanilla SMPLify-X that effectively estimates 3D signs from monocular sign videos. To demonstrate the superior performance of our 3D sign estimator, we benchmark it against three state-of-the-art whole-body estimation methods: SMPLify-X [49], SMPLer-X [3], and OSX [41], with the back-translation results detailed in Table 2. Our approach outperforms all three methods, whether they are optimization-based (SMPLify-X) or regression-based (SMPLer-X and OSX). This improvement results from the incorporation of temporal consistency and prior knowledge of sign languages. Additionally, under the same experimental setting, we introduce a strong baseline that generates 2D keypoints for each frame using a pre-trained HRNet [62], contrasting with our method and other baselines

Dataset	Method	Nat.	Smo.	Sim.
P-2014T	SMPLify-X [49]	1.52	1.98	2.41
	Ours	<b>3.58</b>	<b>4.04</b>	<b>3.94</b>
CSL	SMPLify-X [49]	1.27	1.75	1.69
	Ours	<b>3.78</b>	<b>4.14</b>	<b>3.78</b>

Table 3. User study with deaf participants. Nat.: naturalness; Smo.: smoothness; Sim.: similarity to the raw video. Score range: 1-5.

Method	Fixed Duration	Hand Only	w/o CD	Default
L1 Distance	1.83	1.22	1.34	<b>1.04</b>

Table 4. Ablation study for the sign connector on the Phoenix-2014T dev set. CD: coordinate distance.

that re-project the estimated 3D keypoints back into 2D space. We observe that our approach outperforms this baseline on Phoenix-2014T. This superiority can be attributed to the consideration of temporal consistency.

**User Study with Deaf Participants.** The primary goal of our Spoken2Sign system is to narrow the communication gap between the deaf and the hearing. Consequently, conducting a user study with deaf participants is essential. We invite four signers to evaluate our Spoken2Sign results on three aspects: naturalness (checking for awkward poses), smoothness (observing for noticeable shaking between frames), and similarity to raw videos<sup>1</sup>. We provide 100 randomly selected videos from each dataset to the participants, who then give a rating ranging from 1 to 5 for each aspect. The average ratings across all videos and participants are reported in Table 3. It is evident that our approach significantly outperforms the baseline, SMPLify-X [49], in all aspects.

**Sign Connector.** The objective of our sign connector (see Figure 3) is to predict the duration of the co-articulation between two adjacent 3D signs. The default configuration of our sign connector takes a concatenation of the 3D keypoints of the preceding sign  $\mathcal{D}_{JSC}^{pre}$ , the 3D keypoints of the succeeding sign  $\mathcal{D}_{JSC}^{next}$ , and their coordinate distance  $\mathcal{D}_{JSC}^{pre} - \mathcal{D}_{JSC}^{next}$ , as inputs. In Table 4, we compare this default approach with a baseline, where the duration of each co-articulation is set to a fixed value of 4 (the average duration derived from the training set’s statistics). We also consider two variants: “hand only” and “without coordinate distance” (w/o CD). The “hand only” variant uses only hand keypoints as inputs, while the “w/o CD” variant relies solely on the concatenation of  $\mathcal{D}_{JSC}^{pre}$  and  $\mathcal{D}_{JSC}^{next}$ . For each strategy, we calculate the average L1 distance between the predictions and ground truths across all co-articulations. Our default strategy outperforms all other variants.

<sup>1</sup>Though the participants are not native in German sign language, their familiarity with general sign language rules enables them to evaluate the similarity to sign videos for Phoenix-2014T.

Dataset	3D Keypoint Augmentation	Per-instance		Per-class	
		Top-1	Top-5	Top-1	Top-5
WLASL		46.20	78.81	43.72	77.55
	✓	<b>47.66</b>	<b>79.71</b>	<b>45.10</b>	<b>78.16</b>
MSASL		51.81	73.78	48.52	71.76
	✓	<b>53.10</b>	<b>75.06</b>	<b>49.71</b>	<b>72.71</b>

Table 5. Ablation study on 3D keypoint augmentation.

Dataset	View		Dev		Test	
	Frontal	Side	BLEU-4	ROUGE	BLEU-4	ROUGE
P-2014T	✓		24.16	49.12	25.46	49.68
		✓	22.60	47.31	23.49	47.31
	✓	✓	<b>24.69</b>	<b>50.34</b>	<b>26.54</b>	<b>50.69</b>
CSL	✓		21.66	49.69	21.44	49.80
		✓	20.44	48.31	20.03	48.60
	✓	✓	<b>23.14</b>	<b>52.13</b>	<b>22.22</b>	<b>51.47</b>

Table 6. Ablation study on multi-view Sign2Spoken translation.

### 4.3. Effectiveness of the By-Products

Our approach is able to estimate 3D signs from monocular sign videos. In Section 3.4, we introduce two by-products, 3D keypoint augmentation and multi-view understanding, which have the potential to improve keypoint-based models for sign language understanding.

**3D Keypoint Augmentation.** 3D signs can be rotated at any angle, motivating us to develop 3D keypoint augmentation. This is achieved by randomly rotating the input 3D sign by a small angle before projecting it into 2D space. To validate its effectiveness, we turn to two challenging ISLR datasets, WLASL and MSASL, where the variation of signer poses is more dramatic than that in Phoenix-2014T and CSL-Daily. We use NLA-SLR-Keypoint-64 [80] as the base model. As shown in Table 5, 3D keypoint augmentation consistently improves model performance across all metrics on the dev sets of both datasets, with almost no extra training cost.

**Multi-View Spoken2Sign Translation.** Another by-product is the use of side-view keypoints to enhance the performance of the model trained on frontal-view keypoints. Table 6 shows the effectiveness of multi-view Spoken2Sign translation, with the SingleStream-Keypoint [9] as the base model.

## 5. Conclusion

This paper focuses on Spoken2Sign translation, a reverse process to traditional Sign2Spoken translation, aimed at narrowing the communication gap between deaf and hearing individuals. In contrast to prior works that produce translation results in 2D space, our innovative method generates 3D signs using the proposed techniques such as SMPLSign-X and sign connector. The translation results are displayed through an avatar. Our method involves three main steps: 1) building a sign language dictionary; 2) estimating the 3D representation for each sign in this dictionary; and



3) executing Spoken2Sign translation and rendering an avatar. Additionally, we introduce two by-products, 3D keypoint augmentation and multi-view understanding, which significantly promote the keypoint-based models. Extensive experiments demonstrate the effectiveness of our approach.

## References

- [1] Samuel Albanie, Gül Varol, Liliane Momeni, Triantafyllos Afouras, Joon Son Chung, Neil Fox, and Andrew Zisserman. BSL-1K: Scaling up co-articulated sign language recognition using mouthing cues. In *ECCV*, pages 35–53, 2020. [2](#)
- [2] Jianmin Bao, Dong Chen, Fang Wen, Houqiang Li, and Gang Hua. Cvae-gan: fine-grained image generation through asymmetric training. In *ICCV*, pages 2745–2754, 2017. [1](#)
- [3] Zhongang Cai, Wanqi Yin, Ailing Zeng, Chen Wei, Qingping Sun, Yanjun Wang, Hui En Pang, Haiyi Mei, Mingyuan Zhang, Lei Zhang, et al. Smpner-x: Scaling up expressive human pose and shape estimation. In *NeurIPS*, 2023. [3](#), [7](#), [12](#), [16](#)
- [4] Necati Cihan Camgoz, Simon Hadfield, Oscar Koller, Hermann Ney, and Richard Bowden. Neural sign language translation. In *CVPR*, pages 7784–7793, 2018. [2](#), [3](#), [4](#), [5](#), [6](#), [13](#), [15](#), [16](#), [18](#)
- [5] Necati Cihan Camgoz, Oscar Koller, Simon Hadfield, and Richard Bowden. Multi-channel transformers for multi-articulatory sign language translation. In *ECCV*, pages 301–319. Springer, 2020.
- [6] Necati Cihan Camgöz, Oscar Koller, Simon Hadfield, and Richard Bowden. Sign language transformers: Joint end-to-end sign language recognition and translation. In *CVPR*, pages 10020–10030, 2020. [2](#)
- [7] Ting Chen, Simon Kornblith, Mohammad Norouzi, and Geoffrey Hinton. A simple framework for contrastive learning of visual representations. In *ICML*, pages 1597–1607. PMLR, 2020. [2](#)
- [8] Yutong Chen, Fangyun Wei, Xiao Sun, Zhirong Wu, and Stephen Lin. A simple multi-modality transfer learning baseline for sign language translation. In *CVPR*, pages 5120–5130, 2022. [1](#), [2](#)
- [9] Yutong Chen, Ronglai Zuo, Fangyun Wei, Yu Wu, Shujie Liu, and Brian Mak. Two-stream network for sign language recognition and translation. In *NeurIPS*, 2022. [1](#), [2](#), [3](#), [4](#), [5](#), [8](#), [11](#)
- [10] Ka Leong Cheng, Zhaoyang Yang, Qifeng Chen, and Yu-Wing Tai. Fully convolutional networks for continuous sign language recognition. In *ECCV*, pages 697–714, 2020. [2](#)
- [11] Yiting Cheng, Fangyun Wei, Jianmin Bao, Dong Chen, and Wenqiang Zhang. Cico: Domain-aware sign language retrieval via cross-lingual contrastive learning. In *CVPR*, 2023. [2](#)
- [12] Blender Online Community. *Blender - a 3D modelling and rendering package*. Blender Foundation, Stichting Blender Foundation, Amsterdam, 2018. [5](#)
- [13] Runpeng Cui, Hu Liu, and Changshui Zhang. A deep neural framework for continuous sign language recognition by iterative training. *IEEE TMM*, PP:1–1, 2019. [4](#), [11](#)
- [14] Amanda Duarte, Shruti Palaskar, Lucas Ventura, Deepti Ghadiyaram, Kenneth DeHaan, Florian Metze, Jordi Torres, and Xavier Giro-i Nieto. How2sign: a large-scale multimodal dataset for continuous american sign language. In *CVPR*, pages 2735–2744, 2021. [3](#)
- [15] Amanda Duarte, Samuel Albanie, Xavier Giró-i Nieto, and Gül Varol. Sign language video retrieval with free-form textual queries. In *CVPR*, pages 14094–14104, 2022. [2](#)
- [16] Sen Fang, Chunyu Sui, Xuedong Zhang, and Yapeng Tian. Signdiff: Learning diffusion models for american sign language production, 2023. [1](#), [3](#), [7](#)
- [17] Maria-Paola Forte, Peter Kulits, Chun-Hao P Huang, Vasileios Choutas, Dimitrios Tzionas, Katherine J Kuchenbecker, and Michael J Black. Reconstructing signing avatars from video using linguistic priors. In *CVPR*, pages 12791–12801, 2023. [3](#)
- [18] Stuart Geman. Statistical methods for tomographic image reconstruction. *Bulletin of International Statistical Institute*, 4:5–21, 1987. [4](#)
- [19] Alex Graves, Santiago Fernández, Faustino Gomez, and Jürgen Schmidhuber. Connectionist temporal classification: labelling unsegmented sequence data with recurrent neural networks. In *ICML*, pages 369–376, 2006. [2](#), [4](#)
- [20] Aiming Hao, Yuecong Min, and Xilin Chen. Self-mutual distillation learning for continuous sign language recognition. In *ICCV*, pages 11303–11312, 2021. [2](#)
- [21] Hezhen Hu, Wengang Zhou, and Houqiang Li. Hand-model-aware sign language recognition. In *AAAI*, pages 1558–1566, 2021. [2](#), [3](#)
- [22] Hezhen Hu, Weichao Zhao, Wengang Zhou, and Houqiang Li. Signbert+: Hand-model-aware self-supervised pre-training for sign language understanding. *IEEE TPAMI*, 2023. [2](#), [3](#)
- [23] Lianyu Hu, Liqing Gao, Wei Feng, et al. Self-emphasizing network for continuous sign language recognition. In *AAAI*, 2023. [2](#)
- [24] Lianyu Hu, Liqing Gao, Zekang Liu, and Wei Feng. Continuous sign language recognition with correlation network. In *CVPR*, 2023. [3](#)
- [25] Wencan Huang, Wenwen Pan, Zhou Zhao, and Qi Tian. Towards fast and high-quality sign language production. In *MM*, pages 3172–3181, 2021. [1](#)
- [26] Wencan Huang, Zhou Zhao, Jinzheng He, and Mingmin Zhang. Dualsign: Semi-supervised sign language production with balanced multi-modal multi-task dual transformation. In *MM*, pages 5486–5495, 2022.
- [27] Euijun Hwang, Jung-Ho Kim, and Jong C Park. Non-autoregressive sign language production with gaussian space. In *BMVC*, 2021. [1](#), [3](#)
- [28] Songyao Jiang, Bin Sun, Lichen Wang, Yue Bai, Kunpeng Li, and Yun Fu. Skeleton aware multi-modal sign language recognition. In *CVPRW*, pages 3413–3423, 2021. [2](#)
- [29] Sheng Jin, Lumin Xu, Jin Xu, Can Wang, Wentao Liu, Chen Qian, Wanli Ouyang, and Ping Luo. Whole-body human pose estimation in the wild. In *ECCV*, pages 196–214, 2020. [4](#)
- [30] Hanbyul Joo, Tomas Simon, and Yaser Sheikh. Total capture: A 3d deformation model for tracking faces, hands, and bodies. In *CVPR*, pages 8320–8329, 2018. [2](#), [3](#)

- [31] Hamid Reza Vaezi Joze and Oscar Koller. MS-ASL: A large-scale data set and benchmark for understanding American sign language. In *BMVC*, 2019. 2, 7
- [32] Angjoo Kanazawa, Michael J Black, David W Jacobs, and Jitendra Malik. End-to-end recovery of human shape and pose. In *CVPR*, pages 7122–7131, 2018. 3
- [33] Diederik P. Kingma and Jimmy Ba. Adam: A method for stochastic optimization. In *ICLR*, 2015. 7
- [34] Michael Kipp, Alexis Heloir, and Quan Nguyen. Sign language avatars: Animation and comprehensibility. In *Intelligent Virtual Agents: 10th International Conference, IVA 2011, Reykjavik, Iceland, September 15-17, 2011. Proceedings 11*, pages 113–126. Springer, 2011. 3
- [35] Taku Kudo and John Richardson. Sentencepiece: A simple and language independent subword tokenizer and detokenizer for neural text processing. *arXiv preprint arXiv:1808.06226*, 2018. 11
- [36] Christoph Lassner, Javier Romero, Martin Kiefel, Federica Bogo, Michael J Black, and Peter V Gehler. Unite the people: Closing the loop between 3d and 2d human representations. In *CVPR*, pages 6050–6059, 2017. 3
- [37] Taeryung Lee, Yeonguk Oh, and Kyoung Mu Lee. Human part-wise 3d motion context learning for sign language recognition. In *ICCV*, pages 20740–20750, 2023. 3
- [38] Dongxu Li, Cristian Rodriguez, Xin Yu, and Hongdong Li. Word-level deep sign language recognition from video: A new large-scale dataset and methods comparison. In *WACV*, pages 1459–1469, 2020. 2, 7
- [39] Dongxu Li, Chenchen Xu, Xin Yu, Kaihao Zhang, Benjamin Swift, Hanna Suominen, and Hongdong Li. Tspnet: Hierarchical feature learning via temporal semantic pyramid for sign language translation. In *NeurIPS*, pages 12034–12045, 2020. 1
- [40] Dongxu Li, Xin Yu, Chenchen Xu, Lars Petersson, and Hongdong Li. Transferring cross-domain knowledge for video sign language recognition. In *CVPR*, pages 6205–6214, 2020. 2
- [41] Jing Lin, Ailing Zeng, Haoqian Wang, Lei Zhang, and Yu Li. One-stage 3d whole-body mesh recovery with component aware transformer. In *CVPR*, pages 21159–21168, 2023. 3, 7, 12, 16
- [42] Yinhan Liu, Jiatao Gu, Naman Goyal, Xian Li, Sergey Edunov, Marjan Ghazvininejad, Mike Lewis, and Luke Zettlemoyer. Multilingual denoising pre-training for neural machine translation. *TACL*, 8:726–742, 2020. 2, 3, 5, 11
- [43] John McDonald, Rosalee Wolfe, Jerry Schnepp, Julie Hochgesang, Diana Gorman Jamrozik, Marie Stumbo, Larwan Berke, Melissa Bialek, and Farah Thomas. An automated technique for real-time production of lifelike animations of american sign language. *Universal Access in the Information Society*, 15:551–566, 2016. 3
- [44] Yuecong Min, Aiming Hao, Xiujuan Chai, and Xilin Chen. Visual alignment constraint for continuous sign language recognition. In *ICCV*, pages 11542–11551, 2021. 2
- [45] Liliane Momeni, Gul Varol, Samuel Albanie, Triantafyllos Afouras, and Andrew Zisserman. Watch, read and lookup: learning to spot signs from multiple supervisors. In *ACCV*, 2020. 2
- [46] Liliane Momeni, Hannah Bull, KR Prajwal, Samuel Albanie, Gül Varol, and Andrew Zisserman. Automatic dense annotation of large-vocabulary sign language videos. In *ECCV*, pages 671–690, 2022. 2
- [47] Meinard Müller. Dynamic time warping. *Information retrieval for music and motion*, pages 69–84, 2007. 4, 11
- [48] Jorge Nocedal and Stephen J Wright. Nonlinear equations. *Numerical Optimization*, pages 270–302, 2006. 7
- [49] Georgios Pavlakos, Vasileios Choutas, Nima Ghorbani, Timo Bolkart, Ahmed AA Osman, Dimitrios Tzionas, and Michael J Black. Expressive body capture: 3d hands, face, and body from a single image. In *CVPR*, pages 10975–10985, 2019. 2, 3, 4, 5, 7, 8, 11, 12, 16
- [50] Razieh Rastgoo, Kourosh Kiani, Sergio Escalera, and Mohammad Sabokrou. Sign language production: A review. In *CVPRW*, pages 3451–3461, 2021. 1, 3
- [51] Ali Razavi, Aaron Van den Oord, and Oriol Vinyals. Generating diverse high-fidelity images with vq-vae-2. *NeurIPS*, 32, 2019. 1
- [52] Ben Saunders, Necati Cihan Camgoz, and Richard Bowden. Progressive transformers for end-to-end sign language production. In *ECCV*, pages 687–705, 2020. 1, 3, 5, 7
- [53] Ben Saunders, Necati Cihan Camgöz, and Richard Bowden. Adversarial training for multi-channel sign language production. In *BMVC*, 2020. 1, 3, 5, 7
- [54] Ben Saunders, Necati Cihan Camgoz, and Richard Bowden. Anonymsign: Novel human appearance synthesis for sign language video anonymisation. In *FG 2021*, pages 1–8, 2021. 7
- [55] Ben Saunders, Necati Cihan Camgoz, and Richard Bowden. Continuous 3d multi-channel sign language production via progressive transformers and mixture density networks. *IJCV*, 129(7):2113–2135, 2021. 5, 6, 7
- [56] Ben Saunders, Necati Cihan Camgoz, and Richard Bowden. Mixed signals: Sign language production via a mixture of motion primitives. In *ICCV*, pages 1919–1929, 2021. 1, 3, 7
- [57] Ben Saunders, Necati Cihan Camgoz, and Richard Bowden. Signing at scale: Learning to co-articulate signs for large-scale photo-realistic sign language production. In *CVPR*, pages 5141–5151, 2022. 1, 3, 5, 6, 7, 12
- [58] Konstantin Shmelkov, Cordelia Schmid, and Karteek Alahari. How good is my gan? In *ECCV*, pages 213–229, 2018. 1
- [59] Stephanie Stoll, Necati Cihan Camgoz, Simon Hadfield, and Richard Bowden. Text2sign: towards sign language production using neural machine translation and generative adversarial networks. *IJCV*, 128(4):891–908, 2020. 1, 3
- [60] Shengeng Tang, Richang Hong, Dan Guo, and Meng Wang. Gloss semantic-enhanced network with online back-translation for sign language production. In *MM*, pages 5630–5638, 2022. 1, 3
- [61] Gul Varol, Liliane Momeni, Samuel Albanie, Triantafyllos Afouras, and Andrew Zisserman. Read and attend: Temporal localisation in sign language videos. In *CVPR*, pages 16857–16866, 2021. 2
- [62] Jingdong Wang, Ke Sun, Tianheng Cheng, Borui Jiang, Chaorui Deng, Yang Zhao, Dong Liu, Yadong Mu, Mingkui

Tan, Xinggong Wang, et al. Deep high-resolution representation learning for visual recognition. *IEEE TPAMI*, 43(10): 3349–3364, 2020. 4, 7, 12

[63] Fangyun Wei and Yutong Chen. Improving continuous sign language recognition with cross-lingual signs. In *ICCV*, pages 23612–23621, 2023. 2, 4

[64] Donglai Xiang, Hanbyul Joo, and Yaser Sheikh. Monocular total capture: Posing face, body, and hands in the wild. In *CVPR*, pages 10965–10974, 2019. 3

[65] Pan Xie, Qipeng Zhang, Zexian Li, Hao Tang, Yao Du, and Xiaohui Hu. Vector quantized diffusion model with codeunit for text-to-sign pose sequences generation, 2023. 1, 3

[66] Hongyi Xu, Eduard Gabriel Bazavan, Andrei Zanfir, William T Freeman, Rahul Sukthankar, and Cristian Sminchisescu. Ghum & ghuml: Generative 3d human shape and articulated pose models. In *CVPR*, pages 6184–6193, 2020. 2, 3

[67] Yuanlu Xu, Song-Chun Zhu, and Tony Tung. Denserac: Joint 3d pose and shape estimation by dense render-and-compare. In *ICCV*, pages 7760–7770, 2019. 3

[68] Huijie Yao, Wengang Zhou, Hao Feng, Hezhen Hu, Hao Zhou, and Houqiang Li. Sign language translation with iterative prototype. In *ICCV*, pages 15592–15601, 2023. 1

[69] Aoxiong Yin, Zhou Zhao, Jinglin Liu, WeiKe Jin, Meng Zhang, Xingshan Zeng, and Xiaofei He. Simulst: End-to-end simultaneous sign language translation. In *MM*, pages 4118–4127, 2021. 1

[70] Kayo Yin and Jesse Read. Better sign language translation with stmc-transformer. *COLING*, 2020. 2

[71] Lvmin Zhang, Anyi Rao, and Maneesh Agrawala. Adding conditional control to text-to-image diffusion models. In *ICCV*, pages 3836–3847, 2023. 1, 7

[72] Weichao Zhao, Hezhen Hu, Wengang Zhou, Jiabin Shi, and Houqiang Li. BEST: BERT pre-training for sign language recognition with coupling tokenization. In *AAAI*, 2023. 2

[73] Jiangbin Zheng, Yile Wang, Cheng Tan, Siyuan Li, Ge Wang, Jun Xia, Yidong Chen, and Stan Z Li. CVT-SLR: Contrastive visual-textual transformation for sign language recognition with variational alignment. In *CVPR*, 2023. 2

[74] Benjia Zhou, Zhigang Chen, Albert Clapés, Jun Wan, Yanyan Liang, Sergio Escalera, Zhen Lei, and Du Zhang. Gloss-free sign language translation: Improving from visual-language pretraining. In *ICCV*, pages 20871–20881, 2023. 1

[75] Hao Zhou, Wengang Zhou, Yun Zhou, and Houqiang Li. Spatial-temporal multi-cue network for continuous sign language recognition. In *AAAI*, pages 13009–13016, 2020. 2

[76] Hao Zhou, Wengang Zhou, Weizhen Qi, Junfu Pu, and Houqiang Li. Improving sign language translation with monolingual data by sign back-translation. In *CVPR*, pages 1316–1325, 2021. 2, 4, 5, 6, 14, 15, 16, 18

[77] Hao Zhou, Wengang Zhou, Yun Zhou, and Houqiang Li. Spatial-temporal multi-cue network for sign language recognition and translation. *IEEE TMM*, 24:768–779, 2021. 2

[78] Ronglai Zuo and Brian Mak. C2SLR: Consistency-enhanced continuous sign language recognition. In *CVPR*, pages 5131–5140, 2022. 2

[79] Ronglai Zuo and Brian Mak. Local context-aware self-attention for continuous sign language recognition. In *Proc. Interspeech*, pages 4810–4814, 2022. 2

[80] Ronglai Zuo, Fangyun Wei, and Brian Mak. Natural language-assisted sign language recognition. In *CVPR*, 2023. 2, 5, 7, 8

## A. More Implementation Details

**Dictionary Construction.** As described in Section 3.1 of the main paper, a well-optimized CSLR model, TwoStream-SLR [9], serves as our sign segmentor to segment a given continuous sign into several isolated ones. Below, we formulate the entire process.

Given a continuous sign video  $\mathbf{V}$  with  $T$  frames, and its corresponding ground truth gloss sequence  $\mathbf{g} = (g_1, \dots, g_N)$  containing  $N$  glosses, the probability of an alignment path  $\theta = (\theta_1, \dots, \theta_T)$  with respect to the ground truth  $\mathbf{g}$ , where  $\theta_t \in \{g_i\}_{i=1}^N \cup \{background\}$ , can be calculated by:

$$p(\theta|\mathbf{V}) = \prod_{t=1}^T p_t(\theta_t), \quad (7)$$

where  $p_t(\theta_t)$  denotes the posterior probability of predicting the  $t$ -th frame as class  $\theta_t$ . The optimal path  $\theta^*$  is the one with the maximum probability in the set of all feasible alignment paths  $\mathcal{S}(\mathbf{g})$  with respect to the ground truth  $\mathbf{g}$ :

$$\theta^* = \arg \max_{\theta \in \mathcal{S}(\mathbf{g})} p(\theta|\mathbf{V}). \quad (8)$$

The optimal path  $\theta^*$  can be efficiently identified using the dynamic time warping (DTW) algorithm [13, 47]. Subsequently, we aggregate successive duplicate predictions into a single isolated sign.

**Text2Gloss Translator.** We utilize mBART [42], a pre-trained sequence-to-sequence denoising auto-encoder, as our Text2Gloss translator. This model adopts a standard Transformer architecture, featuring 12 encoder and decoder layers, which ensures a robust contextual understanding. Our mBART model is initialized with the one pre-trained on a large multilingual corpus. To tailor mBART for Text2Gloss translation, we tokenize the gloss sequences and text sentences into sub-word units using the SentencePiece tokenizer [35] and incorporate positional embeddings. We train the model for 80 epochs, starting with an initial learning rate of  $1e - 5$ , and apply a dropout rate of 0.3 and label smoothing with a factor of 0.2 to prevent overfitting.

## B. More Qualitative Results

**Translation Results.** Please refer to the video demos in the supplementary material for additional visualizations. These demos display the ground truth sign videos alongside the baseline, SMPLify-X [49], and our translation results, which

Method	Dev		Test	
	BLEU-4	ROUGE	BLEU-4	ROUGE
Ours	<b>24.16</b>	<b>49.12</b>	<b>25.46</b>	<b>49.68</b>
w/o $\mathcal{L}_{unseen}$	22.57	47.25	23.70	47.62
w/o $\mathcal{L}_{upright}$	23.10	47.93	23.99	48.00
w/o $\mathcal{L}_{smooth}$	23.64	48.50	24.36	48.35

Table 7. Quantitative ablation study on the proposed loss functions:  $\mathcal{L}_{unseen}$ ,  $\mathcal{L}_{upright}$ , and  $\mathcal{L}_{smooth}$ . We report back-translation performance on Phoenix-2014T.

are presented through a sign avatar. We also show several visualization results in Figure 5 and Figure 6 for Phoenix-2014T and CSL-Daily, respectively.

**Sign Connector.** The objective of the sign connector is to predict the length (denoted as  $L$ ) of co-articulations and to mimic these co-articulations by evenly interpolating  $L$  frames between two adjacent signs in the 3D space. We present three generated co-articulations alongside their corresponding ground truths in Figure 7.

**Comparison with Other 3D Sign Estimators.** In the main paper, we present SMPLSign-X, an enhancement of the original SMPLify-X [49], tailored for 3D sign language estimation. In Table 2 of the main paper, we conduct a quantitative comparison with other state-of-the-art 3D sign estimation methods: SMPLify-X [49], SMPLer-X [3], and OSX [41]. Additionally, we further demonstrate qualitative comparisons with these methods as shown in Figure 8. It is evident that our SMPLSign-X produces more visually appealing estimation results compared to all other methods.

### C. Ablation Studies on Loss Functions

In Section 3.2 of the main paper, we introduce three loss functions to facilitate 3D sign estimation:  $\mathcal{L}_{unseen}$  (Eq. 4),  $\mathcal{L}_{upright}$  (Eq. 5), and  $\mathcal{L}_{smooth}$  (Eq. 6).  $\mathcal{L}_{unseen}$  is designed to draw the unseen keypoints closer to those of the rest pose;  $\mathcal{L}_{upright}$  aims to encourage an upright posture in the upper body; and  $\mathcal{L}_{smooth}$  preserves temporal consistency for generating visually appealing results. Below we conduct both quantitative and qualitative ablation studies to validate the effectiveness of these loss functions.

**Quantitative Ablation Study.** We conduct a quantitative ablation study on the loss functions using the back-translation metric [57]. As shown in Table 7, the omission of any loss function leads to a degradation of performance.

**Qualitative Ablation Study.** As depicted in Figures 9, 10, and 11, it is evident that excluding any loss function degrades the estimation results.

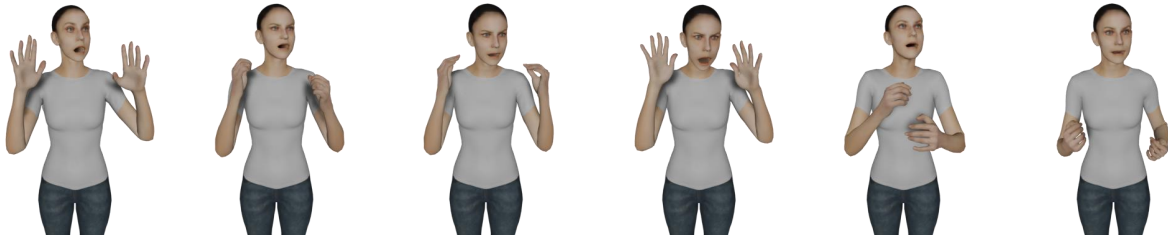
### D. Broader Impacts and Limitations

**Broader Impacts.** For the first time, we introduce a practical system for translating spoken language into sign language, with the translation results presented through a 3D avatar. The Spoken2Sign task is orthogonal and complementary to many sign language understanding tasks, such as sign language recognition and translation. Therefore, our system can further bridge the communication gap between the deaf and the hearing.

**Limitations.** Although we have established a promising baseline for translating spoken languages to sign languages, several limitations still impact the translation results. First, understanding sign languages significantly suffers from the issue of data scarcity. Training on insufficient text-gloss sequence pairs may lead to sub-optimal Text2Gloss models, highlighting the critical need for large-scale sign language datasets. Second, our 3D sign estimator considers 2D keypoints estimated by HRNet [62] as pseudo ground truths. However, inaccurate estimations can result in inferior 3D signs. A 2D keypoint estimator tailored for the sign language field might mitigate this issue. Lastly, as discussed in SMPLify-X [49], accurately estimating 3D skeletons with precise depth from a 2D image remains an unresolved research challenge. Introducing prior knowledge of sign languages could help eliminate depth ambiguity. We leave the resolution of these issues to future research.



(a) "In the south there is a weak wind. In the north it blows moderately on the coasts with strong to stormy gusts."

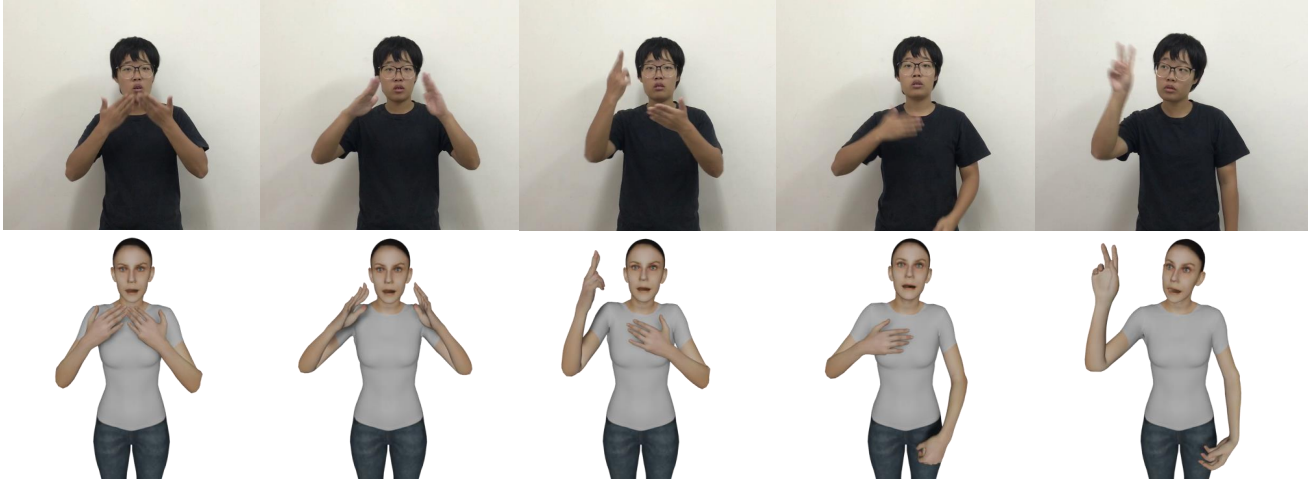


(b) "At night it is mostly cloudy. At first there is only light rain locally, but later it starts to rain heavier in the south."



(c) "There are still a few showers in the northeast, but they subside quickly during the night."

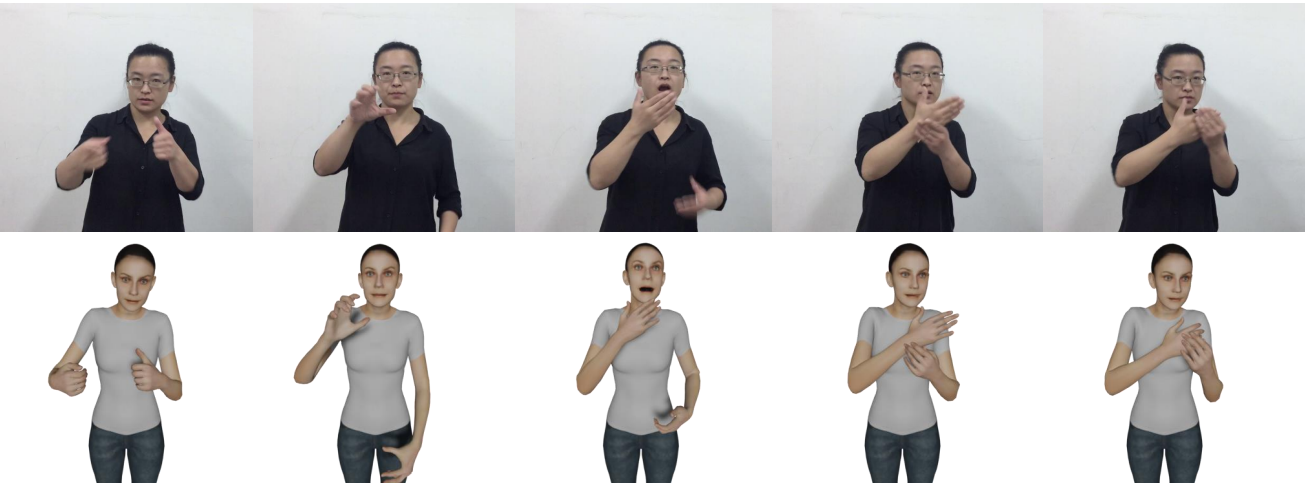
Figure 5. Qualitative results on Phoenix-2014T [4]. In each sub-figure, we display the text in the caption, and show the ground truth sign video and our translation result in the first row and second row, respectively. We translate German into English.



(a) "My mother was sick, and the school allowed me to take leave to go home and visit her."



(b) "My country's education system includes elementary education, vocational education, etc."



(c) "Put the tea and cups away first, and then take out the watermelon from the refrigerator."

Figure 6. Qualitative results on CSL-Daily [76]. In each sub-figure, we display the text in the caption, and show the ground truth sign video and our translation result in the first row and second row, respectively. We translate Chinese into English.



(a) Example (a).



(b) Example (b).



(c) Example (c).

Figure 7. Qualitative comparison between the co-articulations generated by our sign connector and the corresponding ground truth. Three examples are randomly selected from Phoenix-2014T [4] (a and b) and CSL-Daily [76] (c). In each sub-figure, the first row represents the ground truth, and the second row denotes the prediction.

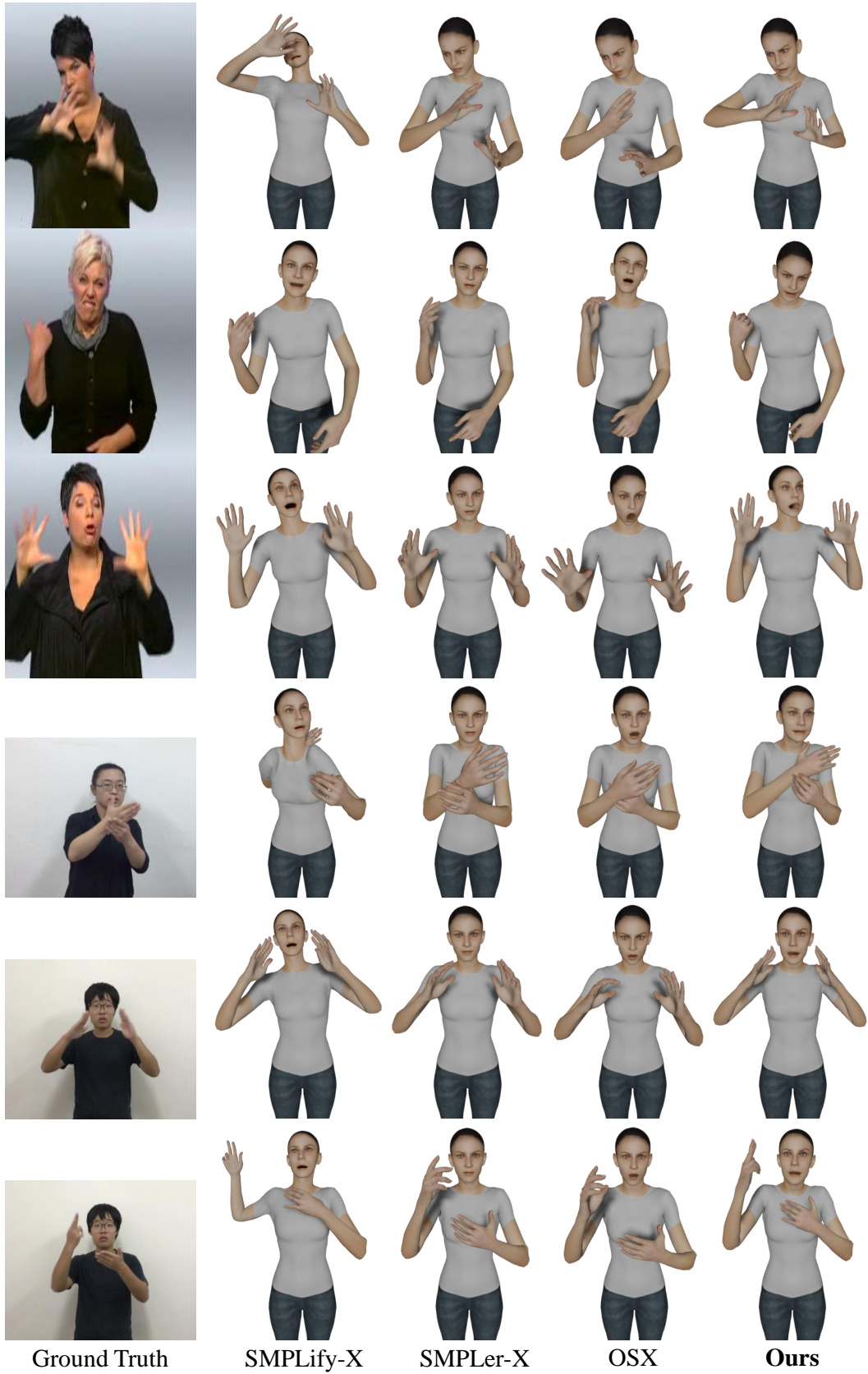


Figure 8. Qualitative comparison with other 3D sign estimation methods including SMPLify-X [49], SMPLer-X [3], and OSX [41], on Phoenix-2014T [4] (the first three rows) and CSL-Daily [76] (the last three rows).



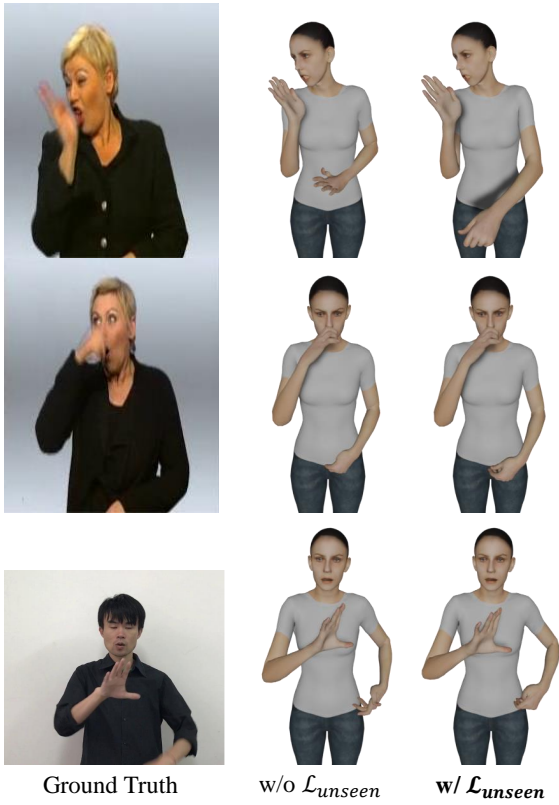


Figure 9. Qualitative ablation study on  $\mathcal{L}_{unseen}$  using Phoenix-2014T (the first two rows) and CSL-Daily (the last row).

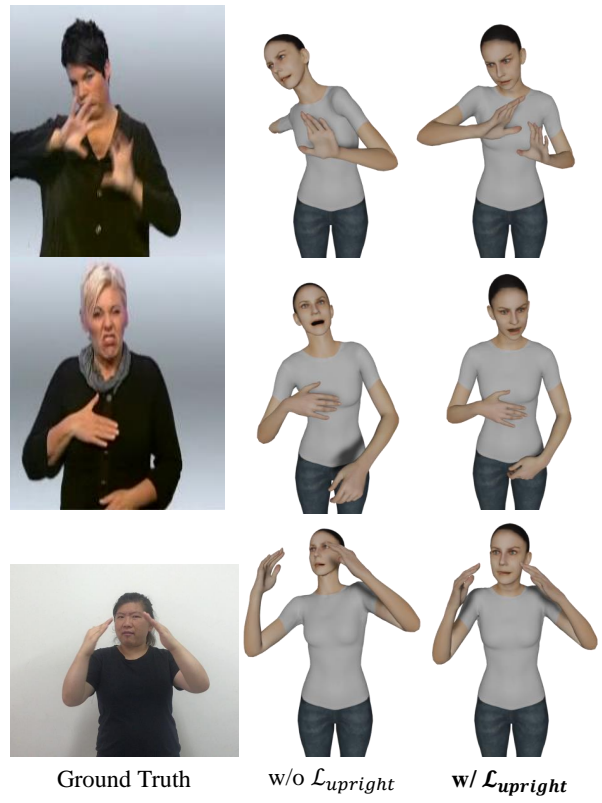


Figure 10. Qualitative ablation study on  $\mathcal{L}_{upright}$  using Phoenix-2014T (the first two rows) and CSL-Daily (the last row).



Figure 11. Qualitative ablation study on  $\mathcal{L}_{smooth}$ . We randomly sample three *consecutive* frames from Phoenix-2014T [4] (the first three columns) and CSL-Daily [76] (the last three columns), respectively.